ECOLOGY LETTERS

Ecology Letters, (2018) **21**: 692–701 doi: 10.1111/ele.12937

LETTER

Bioenergetic theory predicts infection dynamics of human schistosomes in intermediate host snails across ecological gradients

David J. Civitello,[1]* Hiba Fatima,[2] Leah R. Johnson,[3] Roger M. Nisbet[4] and Jason R. Rohr[5]

Abstract

Epidemiological dynamics depend on the traits of hosts and parasites, but hosts and parasites are heterogeneous entities that exist in dynamic environments. Resource availability is a particularly dynamic and potent environmental driver of within-host infection dynamics (temporal patterns of growth, reproduction, parasite production and survival). We developed, parameterised and validated a model for resource-explicit infection dynamics by incorporating a parasitism module into dynamic energy budget theory. The model mechanistically explained the dynamic multivariate responses of the human parasite *Schistosoma mansoni* and its intermediate host snail to variation in resources and host density. At the population level, feedbacks mediated by resource competition could create a unimodal relationship between snail density and human risk of exposure to schistosomes. Consequently, weak snail control could backfire if reductions in snail density release remaining hosts from resource competition. If resource competition is strong and relevant to schistosome production in nature, it could inform control strategies.

Keywords

Density dependence, energy budget, parasite production, parasitism, reproduction, resources.

Ecology Letters (2018) **21**: 692–701

INTRODUCTION

Parasitic diseases of humans and wildlife are emerging and resurging at an unprecedented rate and parasitism can have dramatic effects on ecosystem function, conservation, agriculture and human health (Morens *et al*. 2004; Bekerman & Einav 2015). Indeed, human, livestock and wildlife health are tightly linked because many of the most impactful infectious diseases of humans are vector-borne or zoonotic [i.e. involve a nonhuman host (Wolfe *et al*. 2007)]. Given this strong link between human and wildlife disease, it is critical to understand disease dynamics in nonhuman hosts, especially those that can transmit parasites to humans.

Predicting disease dynamics requires an understanding of the traits of both hosts and parasites. Individual-level traits, such as host susceptibility and parasite reproduction, drive population- and community-level disease dynamics (Anderson & May 1986). However, hosts and parasites are not uniform entities that exist in constant environments. Instead, organisms and the environment are heterogeneous across space and time. Much theory has focused on how infection success and epidemiological dynamics are influenced by intrinsic drivers (e.g. infection genetics or the ability to produce toxins (Agrawal & Lively 2002) or environmental factors (Mordecai *et al*. 2013). A framework that integrates intrinsic and extrinsic drivers could enhance our ability to predict and manage disease outbreaks.

Resource availability is a powerful and dynamic environmental driver of disease. Parasites steal resources from their hosts to fuel their own growth and reproduction. Thus, starving hosts can be resource-limiting environments for parasites (Seppälä *et al*. 2008). Conversely, well-provisioned hosts may deploy energetically costly immune defences (Sheldon & Verhulst 1996). These mechanisms can lead to positive, negative or unimodal (hump-shaped) relationships among host resource acquisition, parasite reproduction, transmission and the virulence of infection (Cressler *et al*. 2014). In natural populations, per capita resource acquisition rates are extremely variable because they depend on resource density and quality, competition among consumers and abiotic factors (Hargrave *et al*. 2011). Bioenergetic theory mechanistically links how organisms acquire and use energy. By formalising the role of hosts and parasites as resource consumers, bioenergetic theory for infection could predict how epidemiological traits respond to the variation in densities of hosts and resources that occurs across space and during epidemics.

Here, we develop bioenergetic theory for infection dynamics using a case study of the human parasite *Schistosoma mansoni* (Sambon) and its snail intermediate host *Biomphalaria glabrata* (Say). More than 250 million humans are infected with schistosomes, which disproportionately harm children (Hotez *et al*. 2014). Humans become infected following contact with cercariae, larval schistosomes released by intermediate snail hosts, in freshwater environments. Cercarial production rates of individual

[1]*Department of Biology, Emory University, 1510 Clifton Rd NE, 30322 Atlanta, GA,USA*
[2]*Global Health Institute, Duke University, Durham, NC, USA*
[3]*Department of Statistics, Virginia Polytechnic Institute and State University, Blacksburg, VA, USA*
[4]*Department of Ecology, Evolution, and Marine Biology, University of California, Santa Barbara, UCSB, 93106 Santa Barbara, CA, USA*
[5]*Department of Integrative Biology, University of South Florida, 4202, East Fowler Ave., 33620 Tampa, FL, USA*
**Correspondence: E-mail: dcivite@emory.edu*

snails depend on key intrinsic and extrinsic factors, for example snail size, resource quantity/quality and population density (Coles 1973; Keas & Esch 1997; Sandland & Minchella 2003). Building from well-tested metabolic theory for free-living organisms (Kooijman 2010), we constructed a model that predicts several quantitative aspects of within-host infection dynamics by explicitly tracking the acquisition and use of resources by snails and parasites. We parameterised the model using an experiment that manipulated food resources and tracked growth, reproduction, parasite production and survival for snail hosts. Finally, we validated the model by simulating infection dynamics for individual hosts experiencing different levels of intraspecific competition and comparing these predictions to the results of another experiment that manipulated host and resource density, and therefore, the intensity of resource competition.

MATERIALS AND METHODS

Model construction

Our model builds on the 'standard' model of Dynamic Energy Budget (DEB) theory for a free-living organism (Kooijman 2010). The model tracks changes in the abundance of food resources in the environment, F, and several host traits: physical length, L (defined here as maximum shell diameter and proportional to the cube root of structural biomass); the scaled density of energy reserves, e; and resources invested in maturity/development, D, and in reproduction, R_H. All quantities are modelled through time for an individual host using coupled differential equations. We added two modules to this standard DEB model to track a within-host population of parasites and host survival respectively. Within each host, we track the change in parasite biomass, P, and the resources invested in parasite reproduction, R_P. To model mortality we follow Gergs & Jager (2014) and introduce a variable representing repairable 'damage', with instantaneous hazard rate assumed proportional to damage. In the Supplement, we present the derivation of dynamic equations for the scaled damage density, δ, and the cumulative mortality hazard, H, for hosts. The model structure is in Fig. 1, Eqs 1–10, state variables and parameters listed in Table S1, subscripts H and P distinguish host and parasite variables and parameters.

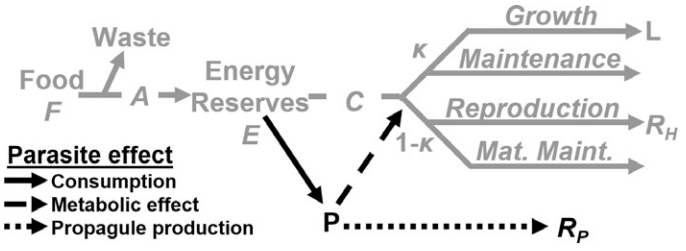

Figure 1 Schematic representation of a dynamic energy budget model (DEB) for a free-living organism (grey) containing a parasite population (black). DEB theory tracks the assimilation, A, of food resources, F, from the environment into energy reserves, E. Energy reserves are then committed, C, to somatic or reproductive processes according to a fixed fraction allocation rule, κ. Once allocated, reserves pay maintenance costs and any energy surpluses fuel increases in structural biomass/biovolume (represented here as length, L) or reproduction, R_H. Here, we introduce a parasite population, P, with three potential effects (black). Parasites consume host reserves (solid line), stealing resources that were destined for host growth and reproduction. Parasites (and/or the host's response to infection) can alter the host's allocation to growth and reproduction (dashed line). Parasites also produce propagules, R_P, that disperse from the host (dotted line).

$$\frac{dF}{dt} = -i_M L^2 f_H \tag{1}$$

$$\frac{dL}{dt} = \frac{gY_{VE}}{3\chi}\left(\frac{\kappa^* a_M e - (m_V + m_R E_M \delta)\chi L}{g+e}\right) \tag{2}$$

$$\frac{de}{dt} = \frac{a_M}{\chi E_M L}(f_H - e) - \frac{i_{PM} f_P}{E_M} p \tag{3}$$

$$\frac{dD}{dt} = \begin{matrix}(1-\kappa^*)C - m_D D & ifD < D_R \\ 0 & ifD \geq D_R\end{matrix} \tag{4}$$

$$\frac{dR_H}{dt} = \begin{matrix}0 & ifD < D_R \\ (1-\kappa^*)C - m_D D & ifD \geq D_R\end{matrix} \tag{5}$$

$$\frac{dP}{dt} = (Y_{PE} i_{PM} f_P (1 - r_P) - m_P)P \tag{6}$$

$$\frac{dR_P}{dt} = \gamma_{RP} Y_{PE} i_{PM} f_P r_P \tag{7}$$

$$\frac{d\delta}{dt} = \frac{\Theta}{\chi L^3}\frac{dR_P}{dt} + k_R(1-e) - k_R\delta - \frac{3\delta}{L}\frac{dL}{dt} \tag{8}$$

$$\frac{dH}{dt} = h_b + h_\delta \max(\delta - \delta_0, 0) \tag{9}$$

$$P(\text{Survival})[t] = e^{-H(t)} \tag{10}$$

Hosts consume food, F, from the external environment at a rate determined by the product of three terms: their maximum surface area-specific ingestion rate, i_M; a Type II functional response, f_H, with half saturation constant, F_h, and their physical length squared (which is proportional to surface area; eqn 1). Hosts assimilate energy from food into an energy 'reserve', with yield of reserves on food Y_{EF}. The maximum assimilation rate, a_M, is the product of the maximum ingestion rate and the yield of reserves on food. Hosts use these reserves to build two types of biomass : structure (which performs vital functions and requires maintenance at rate m_V) and reproductive matter (reserve biomass that has been irreversibly committed to offspring). The reserve dynamics in the absence of parasitism are derived from an assumption of 'weak homeostasis' (Kooijman 2010). Hosts allocate a constant portion, κ, of mobilised reserves, C, to somatic (vs. reproductive) processes. Hosts grow in length based on the energetic costs of growing new structural biomass, determined by the yield of structure on reserves, Y_{VE}, and the difference between energy mobilised for somatic processes and the costs of somatic maintenance and repair (eqn 2). Energy nominally allocated to reproduction is used by juveniles for development, D (eqn 4). Reproduction begins upon achieving the developmental threshold for reproduction, D_R, and developmental status is maintained at the specific rate m_D.

Our model adds a module describing consumption of reserves by a population of parasites (if infected; eqn 3). The module is a parsimonious, general representation of infection

energetics that incorporates several features of snail–schistosome biology (Théron 1981b; a; Kostova & Chipev 1991). Following a seminal DEB model of infection that has been examined qualitatively (Hall *et al.* 2007, 2009), we represent the parasite as a population, rather than as a change to the host's parameter values (e.g. Llandres *et al.* 2015), because schistosomes greatly increase in number during infection. Following infection, parasite biomass (eqn 6) increases through the ingestion and assimilation of host reserves, following a Type II functional response, f_P, with a half saturation coefficient, e_h, maximum mass-specific ingestion rate, i_{PM}, and yield of parasite biomass on host reserve, Y_{PE}. Parasite biomass also decreases through maintenance at a specific rate m_P. A proportion, r_p, of the assimilated reserve is allocated to parasite reproduction, while the rest, $(1–r_p)$, is allocated to parasite biomass growth. A reader with experience in DEB theory should note that this population representation could also be obtained by assuming (1) that individual parasites are 'V1-morphs' (Kooijman 2010), (2) rapid equilibration of reserve density and (3) rapid turnover of reserves. These latter two assumptions parallel those underlying the 'DEBkiss' approximation of standard DEB (Jager *et al.* 2013).

The allocation proportion r_p itself is assumed to increase as a sigmoid function of parasite density within the host, with an inflection point at p_h (Table S1). This parasite allocation function reflects within-host density dependence in parasite growth and limitations of physical space. Furthermore, it influences the timing of parasite reproduction and the maximum density of parasite biomass within host tissue (Gérard *et al.* 1993). Parasite offspring biomass increases from parasite allocation to reproduction, with the relative yield of parasite reproduction biomass on assimilated reserve, γ_{RP}. In addition, infection can modulate the host's realised allocation between soma and reproduction, κ^*, with parasite density-dependent manipulation rate, α, yielding an effective allocation rule, $\kappa^* = \min(\kappa + \alpha P)$. Thus, parasites may affect the host's energy budget in two direct ways: direct consumption of host reserves and by modulating the host's energy allocation rule. If infection diverts host allocation from reproduction to growth, then it can catalyse two widespread phenomena: parasitic castration, the rapid reduction/cessation of reproduction by infected hosts, and host gigantism, increased growth of infected hosts relative to uninfected hosts (Hall *et al.* 2007; Lafferty & Kuris 2009).

We assume that hosts die from damage caused by low energy reserve density, 'reserve depletion', or emerging parasite offspring. Therefore, we implemented extensions of the standard DEB model to account for mild and severe host starvation caused by low reserve density, and linked these extensions to a survival module that tracks mortality risk caused by damage from starvation and parasite emergence based on the stochastic death model of the Generalized Unified Threshold model of Survival (GUTS) framework (Gergs & Jager 2014). Scaled damage density, δ, increases due to the release of parasite offspring with damage intensity, Θ. The damage repair rate, k_R, determines the rate of damage caused by reserve depletion and the damage repair. Damage density also decreases through dilution by growth (eqn 8). Damage repair by hosts may be energetically costly, and we assume that these costs, m_R, are a specified component of somatic maintenance for the host. The cumulative hazard, H, experienced by hosts increases with the background hazard rate, h_b, and a linear function of damage density beyond a threshold, δ_0, with hazard coefficient h_δ (eqn 9). Host survival probability, $P(Survival[t])$ is a negative exponential function of cumulative hazard, H, (eqn 10). Several derived parameters and functions simplify the presentation of the model or the statistical analysis (Table S1). When we fit these models to data (see the Supplement for additional details), we assumed that biomass invested in host or parasite reproduction are immediately released as eggs or parasite propagules, with carbon content per host egg, ε_H, or parasite propagule, ε_P.

Resource supply experiment

We manipulated resource supply rates and tracked the growth, reproduction, parasite production and survival of snail hosts weekly to parameterise our model. We factorially crossed exposure of randomly selected 28-day-old *Biomphalaria glabrata* snails (NMRI strain, length = 4.66 ± 0.05 SE) to parasites (0 or 8 freshly hatched miracidia of *Schistosoma mansoni* [NMRI strain] for 24 h in 5 mL HHCOMBO lake water media) and resource supply rates (0.6875, 1.375, 2.75, 5.5, 11 or 16.5 mg C dry weight per twice-weekly feeding of high quality food). We fed snails a homogenised blend of 6 g dry powdered organic *Spirulina* algae (Now Organics, Bloomingdale, IL, USA) and 6 g fish flakes (Omega One Freshwater Flakes, OmegaSea, Painsville, OH, USA) in 1 g agar dissolved in 100 mL deionised water (diet was 47% C and 10% N; NC2100 Elemental Analyzer, CE Elantech Inc., Lakewood, NJ, USA). The number of replicates per supply rate differed for exposed (n = 16) and unexposed (n = 5) treatments. We excluded exposed hosts from the analysis if they never released cercariae (33% of exposed hosts) because we could not definitively detect successful infection. In almost all cases, visual diagnosis confirmed that these hosts were uninfected. Therefore, these exclusions are unlikely to bias estimates of parasite production from infected hosts. This exclusion resulted in samples sizes of n = 10–12 infected hosts for each resource treatment, which decreased through time as hosts died (see Supplement for additional details).

Resource competition experiment

We followed identical methods as in the resource supply experiment with the following changes. We marked and exposed focal 28-day-old snails (length: 4.30 ± 0.06 SE) and manipulated resource supply rates (5.5, 11 or 16.5 mg C dry weight per feeding) and the abundance of uninfected conspecifics (0, 1, 3, 5 or 7 21-day-old snails, length: 3.76 ± 0.04 SE; due to numerical limitation of 28-day-old individuals, 16 replicates per zero competitor treatment and eight replicates for all other treatments). We also established parasite-free replicates containing 1, 2, 4, 6 or 8 uninfected 21-day-old snails (length 3.47 ± 0.05 SE, four replicates per treatment). We also added three replicates to generate 'replacement' conspecifics for experimental replicates if an uninfected competitor died prior to the focal host (in an infected treatment) or before the end of the experiment (in an unexposed treatment).

This resulted in initial samples sizes of $n = 4$–11 for each treatment with an infected focal host except for the high food – 1 conspecific treatment, which had $n = 1$, and $n = 4$ for all parasite-free replicates ($N = 146$).

Model parameterisation, performance and validation

We parameterised our model of infection dynamics by simulating infections and comparing predictions for host length, cumulative host and parasite reproduction, and host survival simultaneously for each infected and uninfected host in the resource supply experiment in a Bayesian framework (see Supplement for additional details on priors, likelihood model and MCMC sampling). We assessed model performance with the concordance correlation coefficient, r_c (for length, reproduction and parasite production), and the area under the receiver operating characteristic, AUC (for survival), calculated separately for each time series from all observations (i.e. across all individual trajectories; Hanley & McNeil 1982; Lin 1989). We validated the model by challenging it to predict the results of the resource competition experiment in which we factorially manipulated resource availability and the density of uninfected conspecifics for focal infected or uninfected hosts. For the validation step, we simulated life history trajectories for infected focal hosts and uninfected competitors as well as the uninfected groups based on the posterior distribution derived from the first experiment only, with the experimental conditions (host density and resource supply) imposed for each treatment treated as known. Specifically, we modified the food dynamic equation to include depletion of food by all competing hosts according to their size-dependent feeding rates. We calculated r_c and AUC values as above for these *a priori* predictions for each observation. Additionally, to generate our second set of predictions, we refit the model to both data sets simultaneously as described above, which is equivalent to fitting the model to the second experiment using the joint posterior distribution of parameters from the first experiment as the prior for the second, subject to the numerical accuracy of the MCMC (Kruschke 2014). We conducted analyses with replicate MCMC chains after discarding a burn-in. We used thinned chains for computational efficiency to calculate the posterior mean solution for the dynamical system and 99% posterior credible intervals around this mean.

Epidemiological consequences of resource-dependent cercarial production

We used a general epidemiological model to investigate how resource-dependent cercarial production could alter the efficacy of snail control programmes for the control of human risk of exposure. The model, a variant of that in Civitello & Rohr (2014), tracks the densities of resources, R, susceptible snail hosts, S, infected snail hosts, I, and human-infectious cercariae, C, in the aquatic environment:

$$\frac{dR}{dt} = r\left(1 - \frac{R}{K}\right)R - fR(S + I) \tag{11}$$

$$\frac{dS}{dt} = efR(S + \rho I) - dS - \beta SM \tag{12}$$

$$\frac{dI}{dt} = \beta SM - (d + v)I \tag{13}$$

$$\frac{dC}{dt} = \sigma(R)I - mC \tag{14}$$

Resources grow logistically with a maximal growth rate, r, and carrying capacity, K. Resources are consumed by both host classes following a linear functional response with feeding rate f (eqn 11). Susceptible hosts increase based on resource consumption by both host types with conversion efficiency e, and infected hosts exhibit partial castration, with a relative reproductive rate $0 \leq \rho \leq 1$ (eqn 12). Susceptible hosts decrease through background mortality at rate d and infection with miracidia, at constant density M, with transmission rate β. Infected snails increase from transmission and die at an elevated rate due to parasite virulence, v (eqn 13). Free-living cercariae are released into the environment by infected hosts according to a function that may depend on resource density, $\sigma(R)$ (eqn 14). Cercariae die with a background mortality rate, m. We compared two cercarial release functions: constant production, in which release is independent of resources (eqn 15) and resource-dependent production, in which cercarial release is a linear function of resource availability (eqn 16):

$$\sigma(R) = \sigma \tag{15}$$

$$\sigma(R) = \sigma R \tag{16}$$

noting that eqn 16, embodies qualitatively our findings shown in Fig. 2e.

RESULTS

Model parameterisation – resource supply experiment

We parameterised our model with an experiment that manipulated resource availability and tracked the growth, reproduction, parasite production and survival of snail hosts. Across the 24-fold gradient of resource supply rates, final length and reproduction of uninfected snail hosts increased 2.7- and *c*. 6000-fold respectively (Fig. 2a and c). Similarly, final length of infected hosts increased 2.4-fold and lifetime reproduction by infected hosts increased from 0 to *c*. 120 eggs over this gradient (Fig. 2b and d). Cumulative parasite production by infected hosts increased *c*. 60-fold across the supply gradient (Fig. 2e). Survival of uninfected hosts increased with resource supply, but infection increased host mortality (Fig. 2f and g). The fitted bioenergetic model explained the vast majority of variation in these quantities (see Fig. S1 and Table S2 for marginal posterior distributions and highest posterior density estimates of all parameters). Concordance correlation coefficients, r_c, spanned 0.75–0.98 for the growth, reproduction and parasite production time series. The model predicted more rapid mortality of infected hosts than was observed, which likely reflects the compromise of fitting seven time series simultaneously. Nonetheless, AUC values for host survival were moderate, spanning 0.75–0.81 (Fig. 2). Infection permanently reduced snail reproduction, but it temporarily boosted growth relative to uninfected hosts (Figs 2, S2). Ultimately, however, infected hosts were smaller than uninfected hosts.

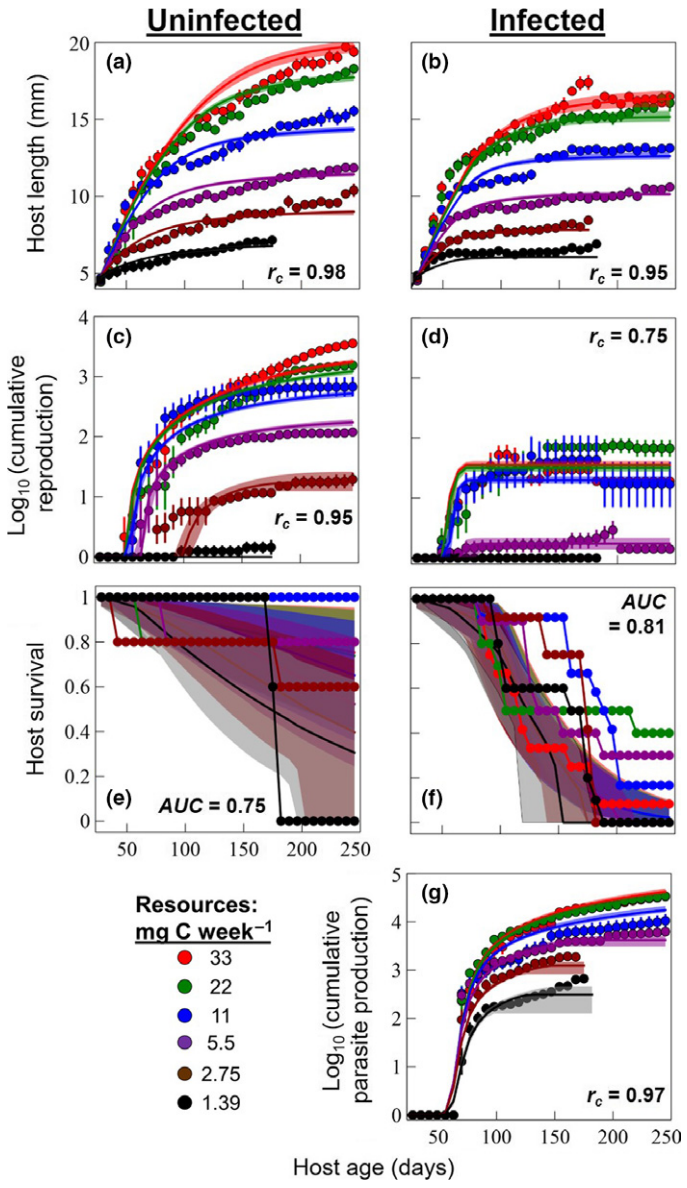

Figure 2 Resource-dependent life history and infection dynamics in an experiment manipulating resource supply rate (colours) and infection status (columns) for individual hosts. Prediction lines and shaded envelopes correspond to the mean and 99% posterior distribution of the mean dynamics of the bioenergetic model. For clarity, data points correspond to treatment means ± SE, although the model was fit to the individual observations. Growth (a) and cumulative reproduction (c) of uninfected hosts increased substantially over the 24-fold resource supply gradient, with *c*. 3- and 6000-fold increases respectively. Host survival increased with resource supply (e), and infection increased host mortality in all but the lowest resource supply treatments (f). Infected host growth, reproduction and parasite production also increased substantially over the resource gradient, by approximately 2.5-fold, from 0 to 120 offspring, and 60-fold, respectively (b, d, g). The model explains these dynamics extremely well, with all r_c = 0.75–0.98, and AUC = 0.75–0.81; however, it predicted more rapid mortality of infected hosts than we observed, especially for low resource supply treatments (F).

Model validation – resource competition experiment

Parameterised with the resource supply experiment, the model predicted strong indirect negative effects of host density on host growth, reproduction and parasite production that are enhanced under low resource supply rates (Fig. S3). The results of the experiment echoed these predictions. For example, cercarial production increased with resource supply, yet competition from up to seven uninfected conspecifics reduced lifetime cercarial production of focal hosts by *c*. 40-fold relative to the competitor-free treatments in the lowest supply rate (Fig. 3d) and *c*. 20-fold under higher supply rates (Fig. 3e–f). There were similarly strong effects of resource supply and competition on host growth and reproduction (Fig. S3), as well as growth and reproduction by infection-free control groups (Fig. S3). These predictions matched the observed infection dynamics well, the AUC was high for host survival (AUC = 0.78), and r_c values were high for host growth (all $r_c \geq 0.87$) and moderate for cercarial production (r_c = 0.76) and host reproduction (r_c = 0.64–0.79; Fig S3).

Fitting the model to the resource supply and resource competition experiments jointly improved the match to the data, and r_c values for infected hosts improved to 0.89 for growth, 0.94 for cercarial production and 0.68 for reproduction, while AUC increased to 0.89 for survival (Fig. 3). Model predictions for the dynamics of growth (r_c = 0.93) and reproduction (r_c = 0.78) by unexposed snail hosts also improved (Fig. S4; see Fig. S1 for marginal posterior distributions of parameters). Despite changes to some parameter estimates, this parameterisation retained an extremely strong fit to the resource supply experiment (Fig. S5).

Epidemiological consequences of resource-dependent cercarial production

The constant production and resource-dependent production model variants both yield analytically tractable equilibria. For both models, the equilibria for R, S, and I are identical (eqs 17–19):

$$R^* = \frac{(d+v)(d+M\beta)}{ef(d+v+M\beta\rho)} \tag{17}$$

$$S^* = \frac{r(d+v)((efK-d-M\beta)(d+v)+efKM\beta\rho)}{ef^2K(d+v+M\beta)(d+v+M\beta\rho)} \tag{18}$$

$$I^* = \frac{rM\beta((efK-d-M\beta)(d+v)+efKM\beta\rho)}{ef^2K(d+v+M\beta)(d+v+M\beta\rho)} \tag{19}$$

For the constant-production model, C^* (Eq. 20) follows in direct proportion from the density of infected hosts:

$$C^*_{CP} = \frac{\sigma rM\beta((efK-d-M\beta)(d+v)+efKM\beta\rho)}{mef^2K(d+v+M\beta)(d+v+M\beta\rho)} = \frac{\sigma}{m}I^* \tag{20}$$

In contrast, for the resource-dependent production model, C^* (eqn 21) becomes a function of both I^* and R^*:

$$C^*_{RDP} = \frac{\sigma rM\beta(d+v)(d+M\beta)((efK-d-M\beta)(d+v)+efKM\beta\rho)}{e^2f^3Km(d+v+M\beta)(d+v+M\beta\rho)^2} = \frac{\sigma}{m}I^*R^* \tag{21}$$

The equilibrium density of resource, R^*, drives the unimodal response of cercarial density to snail control, because R^* itself is a unimodal function of host background death rates. The equilibrium density of cercariae, C^*, is maximised

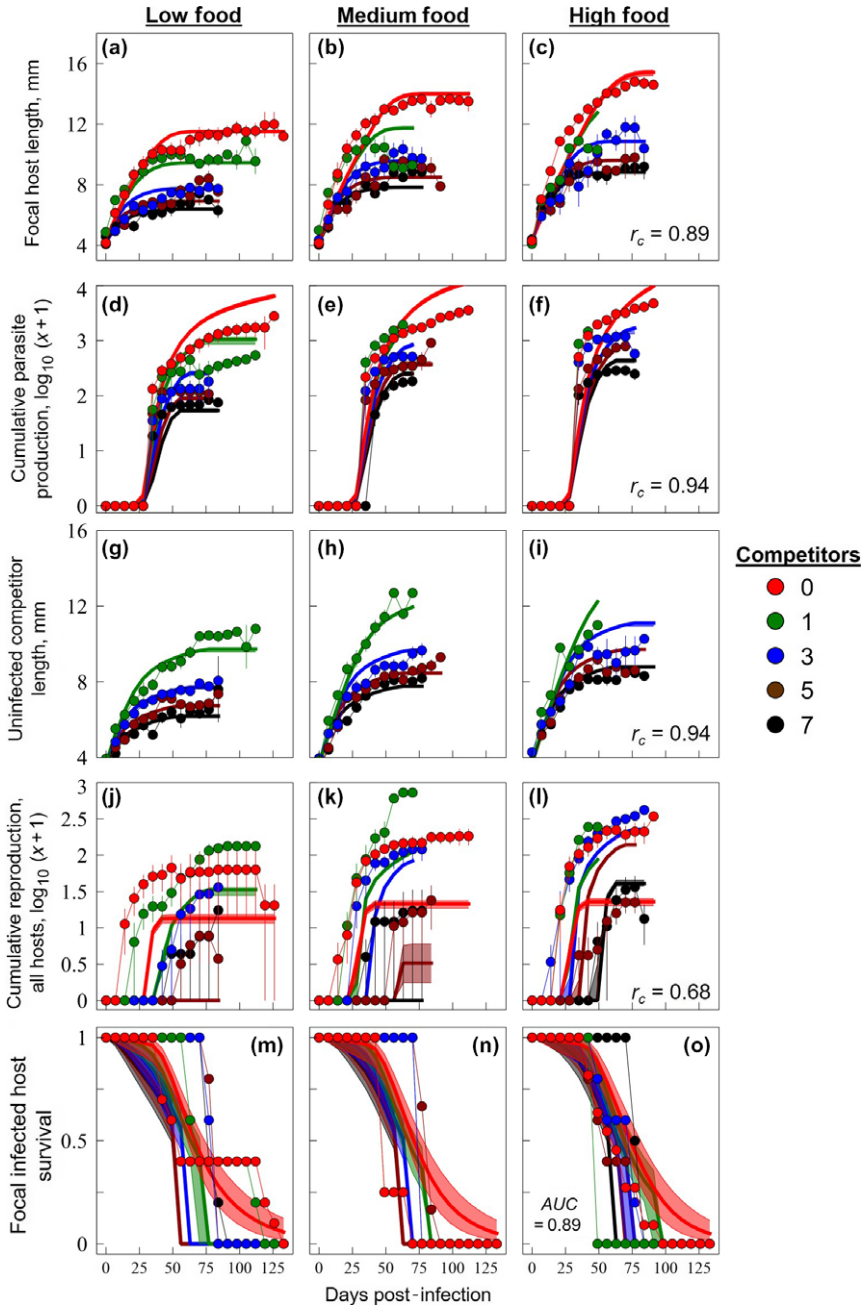

Figure 3 Host density- and resource-dependent infection dynamics in an experiment manipulating uninfected competitor density (colours) and resource supply rates (columns). Prediction lines and envelopes correspond to the mean and 99% posterior distribution of the mean dynamics based on the fitting of the bioenergetic model to this experiment using the posterior distributions of the parameters from the resource gradient experiment as priors. For clarity, data points correspond to treatment means ± SE, although the model was fit to the individual observations. Growth of infected focal hosts (a–c), parasite production by focal hosts (d–f), growth of competitors (g–i) and reproduction by all hosts (j–l) all increased with resource supply but decreased with competitor density. The survival of focal infected hosts (m–o) was similar across the resource and competitor density gradients. The parameterised model predicted growth, parasite production and survival extremely well (all $r_c \geq 0.89$, $AUC = 0.89$). The model predicted total reproduction slightly less successfully (j–l), especially at the lowest resource supply (J), but still agreed well with the observed dynamics ($r_c = 0.68$).

at an intermediate background death rate, d^* (Fig. 4) which cannot be calculated explicitly.

DISCUSSION

Resource acquisition drives tremendous variation in life history and infection dynamics. In the resource supply experiment, lifetime production of human-infectious cercariae by infected snails increased approximately 60-fold over the 24-fold gradient. The fitted bioenergetic model explained much of the variation in these dynamic multivariate (length, reproduction, parasite production and survival) responses (Fig. 2). The positive resource–parasite production pattern observed here and the strong explanatory power of the model suggest

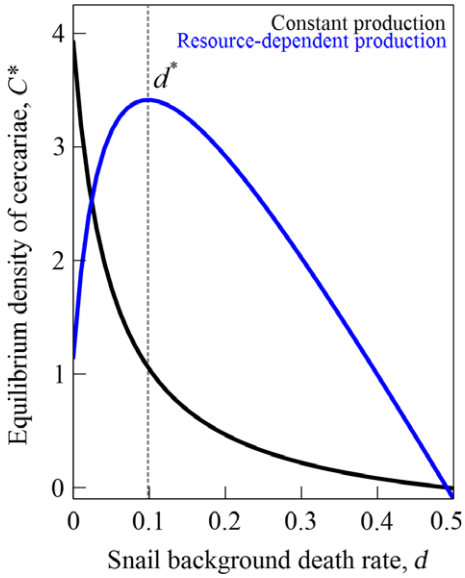

Figure 4 Equilibrium density of human-infectious cercariae, C^*, in a general epidemiological model for human schistosome infections in aquatic snail populations under two models of cercarial production by infected snails: constant production (black) and resource-dependent production (blue). Under the constant-production model, C^* always decreases as snail death rates increase. However, under the resource-dependent production model, C^* responds unimodally to increases in snail death rates, and it peaks again at an intermediate death rate, d^*. If background death rates are high enough, C^* approaches zero because snail populations go extinct. Parameter values used for plotting both models: $r = 1$, $K = 1$, $f = 1$, $e = 0.5$, $M = 1$, $\nu = 0.04$, $\beta = 0.01$, $\rho = 0.1$ and $m = 1$. To better match per snail rates of cercarial production and the scale of plotted values between the two models, we set $\sigma = 20$ for the constant-production model and $\sigma = 300$ for the resource-dependent production model.

that resources, rather than the deployment of costly immune defence (which is not explicitly included in this model, and often generates negative resource-parasite production relationships; Cressler *et al.* 2014), primarily drive variation in parasite success. Indeed, successful *S. mansoni* infections evade haemocyte responses of snails that are induced by other parasites (Loker & Adema 1995; Zahoor *et al.* 2008). In other systems, resource-dependent immune defences may play a critical role in infection dynamics across resource, size or ontogenetic gradients (Cressler *et al.* 2014).

Explicitly adding induced immunity to bioenergetic models could help understand infection dynamics in systems demonstrating potent and costly host defences, but the consistency of our model with observations demonstrates that this seems unnecessary for the specific combination of *B. glabrata* and *S. mansoni* used in this study. However, these strains have been maintained for > 50 years and may have been selected for high parasite productivity. Other snail genotypes or species might exhibit greater constitutive or induced resistance to infection by local schistosomes. If snails in natural populations can induce costly and effective immune defences, then incorporating the energetics of immunity would be important for predictions in field settings because it can qualitatively change the relationship between resource supply and cercarial production. There is genetic variation among snails in the ability to rapidly encapsulate and kill invading schistosome miracidia with haemocytes, primary immune effector cells (Lockyer *et al.* 2012). However, in another *B. glabarata* strain (Salvador), starvation increases hemocyte concentrations and does not reduce resistance (Nelson *et al.* 2016). Additionally, the ability to evade or suppress the induction of snail cellular and humoral defences is a common feature of successful trematode parasites (Coustau *et al.* 2015), which suggests that variation in snail immunity may be more important in determining the probability of infection, but not infection dynamics. It could also explain why parasite production increases with resource supply in many natural snail–trematode combinations (Keas & Esch 1997; Sandland & Minchella 2003; Seppälä *et al.* 2008). Nonetheless, genetic variation in bioenergetic parameters could identify physiological strategies exploited by coevolving schistosomes and snails (Ibikounlé *et al.* 2012).

Flatworms such as schistosomes can cause gigantism, castration and death of their snail hosts (Lafferty & Kuris 2009). This bioenergetic model suggests that these effects emerge from parasite strategies of consumption, manipulation and reproduction. Here, we focus on the parameter estimates derived from fitting both experiments, because these estimates incorporate all accumulated data. Schistosomes consume *c.* 34% of their biomass in reserve per day, efficiently build and maintain biomass ($Y_{PE} \approx 0.88$ and $m_P \approx 0.017$ d^{-1}), and cercarial release harms hosts ($\Theta \approx 2160$; Fig. S1, Table S2). The parasite appears to produce cercariae inefficiently, $\gamma_{RP} \approx 0.05$, but this parameter relates cumulative predictions to cumulative counts observed during 2-hour 'shedding' intervals each week. Therefore, this parameter underestimates true efficiency of parasite reproduction. Consumption of host reserves by parasites can eliminate host reproduction, and it should consistently reduce host growth (Hall *et al.* 2007). However, the temporary gigantism of infected hosts is consistent with an infection-induced shift in the host's allocation strategy towards somatic processes and away from reproduction, which facilitates a brief period of increased host growth before the parasite slows host growth by significantly depleting host reserves (see Supplement for additional details on both parameter sets).

We validated the bioenergetic model by challenging it to predict the results of a second experiment (i.e. predict dynamics to which the model had not been fitted) in which we factorially manipulated resource availability and the density of uninfected conspecifics. Resource competition among hosts decreases per capita consumption by hosts and therefore should predictably reduce growth, reproduction and parasite production. To test this, we first simulated infections in focal snails that shared the same pool of food resources with an increasing number of uninfected conspecifics using parameter sets drawn from the posterior distribution generated from the first (resource supply) experiment. This generated quantitative *a priori* predictions from the model that we could then compare to observed data from this second (resource competition) experiment where we manipulated host density and resource supply rates and quantified host traits and parasite production. Strong predictive ability of the model would indicate

that it captures the mechanistic drivers of host density dependence. Conversely, poor model performance would indicate that resource competition among hosts is relatively unimportant or that physiological rates depend on host density in other ways that are not included in our current model, thereby precluding its use for scaling up to the population level or extrapolating across ecological contexts.

The parameterised model predicted the growth of infected and competing hosts very well (all $r_c \geq 0.87$). The model also predicted variation in cercarial production ($r_c = 0.76$) and host survival ($AUC = 0.78$; Fig. S3) moderately well. Thus, there was a very good match between the model and the observed data, especially given that these are *a priori* predictions, not model fitting, to a novel ecological context. As expected, directly fitting the model simultaneously to the results of both experiments improved the match to the multivariate dynamics for infected and uninfected snails (Fig. 3), while retaining an extremely strong fit to the resource supply experiment (Fig. S5). These results indicate that exploitative resource competition is a dominant driver of infection dynamics across host density gradients because it reduces per capita resource acquisition rates of hosts. The relative importance of other aspects of competition, for example interference competition, size asymmetry, degradation of environmental quality or 'crowding stress', could also be assessed with extensions of this model or supplementary experiments (see Supplement). This within-host model could be fused with a transmission model to generate a fully dynamic model for the aquatic ecology of schistosomes. Snail infection depends on contact with miracidia and per-miracidia susceptibility (Civitello & Rohr 2014). Intrinsic and extrinsic factors, for example genotype, host size/age, exposure time and temperature shape both of these processes (Anderson *et al.* 2009; Théron *et al.* 2014). Therefore, a stochastic transmission model, in which transmission depends on intrinsic or extrinsic factors, could extend this bioenergetic model by specifying the probability of parasite biomass 'arriving' in an individual.

Infection outcomes that depend on resource and host density could have important consequences for epidemiological dynamics and human risk of parasite exposure, which can enhance predictions and management of disease. There can be tremendous variation in resource and host densities across space (Civitello *et al.* 2015) and parasites themselves can depress host densities and alter resource flow and abundance (Hudson *et al.* 1998; Sato *et al.* 2011). Thus, resource-dependent traits could drive epidemiological dynamics and human risk in otherwise unanticipated ways. The density and infectivity of schistosome cercariae in the aquatic environment drives ecological risk for human exposure to schistosomes (Prentice & Ouma 1984). In practice, however, it can be logistically challenging and prohibitively expensive to assess the density of infectious cercariae under field conditions at relevant scales (Ouma *et al.* 1989; Hung & Remais 2008). Instead, management strategies and epidemiological models often assume that cercarial production per snail is constant, and therefore human risk is positively correlated with the density of infected snails (Mangal *et al.* 2008; Sokolow *et al.* 2015). However, densities of cercariae and infected snails can be poorly correlated (Ouma *et al.* 1989; Muhoho *et al.* 1997) and the proportion of infected snails actively releasing cercariae is extremely variable (Hamburger *et al.* 2004), compromising field estimation and model prediction of human risk.

This bioenergetic perspective suggests variation in resource availability and competition could mechanistically explain part of this mismatch and enhance risk assessment. In particular, total cercarial production by snail populations (and therefore ecological risk of human exposure) could be low when snail densities are low (because there are few infected snails) or when snail densities are high (if competition limits per capita parasite production). This potential unimodal relationship between snail density and human risk of exposure could drive the success or failure of current and proposed methods of schistosome control, which depend on reducing the density of snail vectors through molluscicides or predatory biocontrol (Kariuki *et al.* 2013; Sokolow *et al.* 2015). If resource competition in natural snail populations is strong enough, then snail reduction programmes could potentially backfire because decreases in intermediate host density could release remaining hosts from resource competition, boosting per host rates of parasite production (Fig. 4). This effect echoes overcompensation in age-structured models, where increased mortality rates can counterintuitively raise the densities of specific life stages or the total population (Schröder *et al.* 2014). In stage-structured models, overcompensation can occur because increased death rates reduce competition for a shared resource, boosting the resource-dependent reproductive rates of surviving individuals. Overcompensatory effects have been observed in plant and animal systems, and they may explain why efforts to control pest species can backfire (Zipkin *et al.* 2009). Resource-dependent production of cercariae by snail hosts raises the possibility of similar complications for the control of human schistosomes. However, this potential failure of control depends on the intensity of snail control. If snail control increases death rates sufficiently, then it can reduce cercarial densities or even extirpate snail populations, thereby reducing ecological risk of human exposure (Fig. 4).

More quantitative data on resource availability, snail densities and sizes, and cercarial production rates by infected snails in natural transmission sites are still needed to assess the importance of resource competition among snail hosts for control of human risk of exposure to schistosomes. Therefore, we encourage snail monitoring and elimination programmes to estimate per capita schistosome release rates or the starvation times of field-collected snails whenever possible. We also call for population-level models, experiments and field surveys to assess the importance of these ecological feedbacks for epidemiological dynamics and human risk of exposure to schistosomes at the population level and across disease systems more broadly.

ACKNOWLEDGEMENTS

Savannah Poor and Karena Nguyen assisted with the data collection. David Lewis and Bert Anderson conducted the elemental analyses on snail food. Snails and schistosomes were obtained through BEI Resources, NIAID, NIH. DJC was supported by an NIH NRSA postdoctoral fellowship F32AI112255. RMN was supported by US EPA STAR grant 835797. LRJ was supported by NSF PLR 1341649.

AUTHORSHIP

DJC, RMN and JRR conceived the study, DJC and HF conducted the experiments, DJC, LRJ, RMN and JRR developed the analysis, DJC wrote the paper, and all authors edited it.

REFERENCES

Agrawal, A. & Lively, C.M. (2002). Infection genetics: gene-for-gene versus matching-alleles models and all points in between. *Evol. Ecol. Res.*, 4, 79–90.

Anderson, R.M. & May, R.M. (1986). The invasion, persistence and spread of infectious disease within animal and plant communities. *Philos. Trans. R. Soc. Lond. Ser. B-Biol. Sci.*, 314, 533–570.

Anderson, R.M., Mercer, J.G., Wilson, R.A. & Carter, N.P. (2009). Transmission of Schistosoma mansoni from man to snail: experimental studies of miracidial survival and infectivity in relation to larval age, water temperature, host size and host age. *Parasitology*, 85, 339–360.

Bekerman, E. & Einav, S. (2015). Combating emerging viral threats. *Science*, 348, 282–283.

Civitello, D.J. & Rohr, J.R. (2014). Disentangling the effects of exposure and susceptibility on transmission of the zoonotic parasite *Schistosoma mansoni*. *J. Anim. Ecol.*, 83, 1379–1386.

Civitello, D.J., Penczykowski, R.M., Smith, A.N., Shocket, M.S., Duffy, M.A. & Hall, S.R. (2015). Resources, key traits and the size of fungal epidemics in *Daphnia* populations. *J. Anim. Ecol.*, 84, 1010–1017.

Coles, G.C. (1973). Effect of diet and crowding on shedding of *Schistosoma mansoni* cercariae by Biomphalaria glabrata. *Ann. Trop. Med. Parasitol.*, 67, 419–423.

Coustau, C., Gourbal, B., Duval, D., Yoshino, T.P., Adema, C.M. & Mitta, G. (2015). Advances in gastropod immunity from the study of the interaction between the snail *Biomphalaria glabrata* and its parasites: a review of research progress over the last decade. *Fish Shellfish Immunol.*, 46, 5–16.

Cressler, C.E., Nelson, W.A., Day, T. & McCauley, E. (2014). Disentangling the interaction among host resources, the immune system and pathogens. *Ecol. Lett.*, 17, 284–293.

Gérard, C., Moné, H. & Théron, A. (1993). *Schistosoma mansoni – Biomphalaria glabrata*: dynamics of the sporocyst population in relation to the miracidial dose and the host size. *Can. J. Zool.*, 71, 1880–1885.

Gergs, A. & Jager, T. (2014). Body size-mediated starvation resistance in an insect predator. *J. Anim. Ecol.*, 83, 758–768.

Hall, S.R., Becker, C. & Cáceres, C.E. (2007). Parasitic castration: a perspective from a model of dynamic energy budgets. *Integr. Comp. Biol.*, 47, 295–309.

Hall, S.R., Simonis, J.L., Nisbet, R.M., Tessier, A.J. & Caceres, C.E. (2009). Resource ecology of virulence in a planktonic host-parasite system: an explanation using dynamic energy budgets. *Am. Nat.*, 174, 149–162.

Hamburger, J., Hoffman, O., Kariuki, H., Muchiri, E., Ouma, J., Koech, D. *et al.* (2004). Large-scale, polymerase chain reaction-based surveillance of *Schistosoma haematobium* DNA in snails from transmission sites in coastal Kenya: a new tool for studying the dynamics of snail infection. *Am. J. Trop. Med. Hyg.*, 71, 765–773.

Hanley, J.A. & McNeil, B.J. (1982). The meaning and use of the area under a receiver operating characteristic (ROC) curve. *Radiology*, 143, 29–36.

Hargrave, C.W., Hambright, K.D. & Weider, L.J. (2011). Variation in resource consumption across a gradient of increasing intra- and interspecific richness. *Ecology*, 92, 1226–1235.

Hotez, P.J., Alvarado, M., Basáñez, M.-G., Bolliger, I., Bourne, R., Boussinesq, M. *et al.* (2014). The global burden of disease study 2010: interpretation and implications for the neglected tropical diseases. *PLoS Negl. Trop Dis.*, 8, e2865.

Hudson, P.J., Dobson, A.P. & Newborn, D. (1998). Prevention of population cycles by parasite removal. *Science*, 282, 2256–2258.

Hung, Y.W. & Remais, J. (2008). Quantitative detection of *Schistosoma japonicum* cercariae in water by real-time PCR. *PLoS Negl. Trop Dis.*, 2, e337.

Ibikounlé, M., Mouahid, G., Mintsa Nguéma, R., Sakiti, N.G., Kindé-Gasard, D., Massougbodji, A. *et al.* (2012). Life-history traits indicate local adaptation of the schistosome parasite, *Schistosoma mansoni*, to its snail host, *Biomphalaria pfeifferi*. *Exp. Parasitol.*, 132, 501–507.

Jager, T., Martin, B.T. & Zimmer, E.I. (2013). DEBkiss or the quest for the simplest generic model of animal life history. *J. Theor. Biol.*, 328, 9–18.

Kariuki, H.C., Madsen, H., Ouma, J.H., Butterworth, A.E., Dunne, D.W., Booth, M. *et al.* (2013). Long term study on the effect of mollusciciding with niclosamide in stream habitats on the transmission of *Schistosomiasis mansoni* after community-based chemotherapy in Makueni District, Kenya. *Parasites Vectors*, 6, 11.

Keas, B.E. & Esch, G.W. (1997). The effect of diet and reproductive maturity on the growth and reproduction of *Helisoma anceps* (Pulmonata) infected by *Halipegus occidualis* (Trematoda). *J. Parasitol.*, 83, 96–104.

Kooijman, S.A.L.M. (2010). *Dynamic Energy Budget Theory for Metabolic Organisation*. Cambridge university press; Cambridge, UK.

Kostova, T.V. & Chipev, N.H. (1991). A model of the dynamics of intramolluscan trematode populations: some problems concerning oscillatory behavior. *Comput. Math. Appl.*, 21, 1–15.

Kruschke, J. (2014). *Doing Bayesian data analysis: a tutorial with R, JAGS, and Stan*. Academic Press, El Sevier, London.

Lafferty, K.D. & Kuris, A.M. (2009). Parasitic castration: the evolution and ecology of body snatchers. *Trends Parasitol.*, 25, 564–572.

Lin, L.I. (1989). A concordance correlation coefficient to evaluate reproducibility. *Biometrics*, 45, 255–268.

Llandres, A.L., Marques, G.M., Maino, J.L., Kooijman, S., Kearney, M.R. & Casas, J. (2015). A dynamic energy budget for the whole life-cycle of holometabolous insects. *Ecol. Monogr.*, 85, 353–371.

Lockyer, A.E., Emery, A.M., Kane, R.A., Walker, A.J., Mayer, C.D., Mitta, G. *et al.* (2012). Early differential gene expression in haemocytes from resistant and susceptible *Biomphalaria glabrata* strains in response to *Schistosoma mansoni*. *PLoS ONE*, 7, e51102.

Loker, E.S. & Adema, C.M. (1995). Schistosomes, echinostomes and snails: comparative immunobiology. *Parasitology Today*, 11, 120–124.

Mangal, T.D., Paterson, S. & Fenton, A. (2008). Predicting the impact of long-term temperature changes on the epidemiology and control of schistosomiasis: a mechanistic model. *PLoS ONE*, 3, 9.

Mordecai, E.A., Paaijmans, K.P., Johnson, L.R., Balzer, C., Ben-Horin, T., Moor, E. *et al.* (2013). Optimal temperature for malaria transmission is dramatically lower than previously predicted. *Ecol. Lett.*, 16, 22–30.

Morens, D.M., Folkers, G.K. & Fauci, A.S. (2004). The challenge of emerging and re-emerging infectious diseases. *Nature*, 430, 242–249.

Muhoho, N.D., Katsumata, T., Kimura, E., Migwi, D.K., Mutua, W.R., Kiliku, F.M. *et al.* (1997). Cercarial density in the river of an endemic area of schistosomiasis haematobia in Kenya. *Am. J. Trop. Med. Hyg.*, 57, 162–167.

Nelson, M.K., Cruz, B.C., Buena, K.L., Nguyen, H. & Sullivan, J.T. (2016). Effects of abnormal temperature and starvation on the internal defense system of the schistosome-transmitting snail Biomphalaria glabrata. *J. Invertebr. Pathol.*, 138, 18–23.

Ouma, J.H., Sturrock, R.F., Klumpp, R.K. & Kariuki, H.C. (1989). A comparative evaluation of snail sampling and cercariometry to detect *Schistosoma mansoni* transmission in a large-scale, longitudinal field-study in Machakos, Kenya. *Parasitology*, 99(Pt 3), 349–355.

Prentice, M.A. & Ouma, J.H. (1984). Field comparison of mouse immersion and cercariometry for assessing the transmission potential of water containing cercariae of *Schistosoma mansoni*. *Ann. Trop. Med. Parasitol.*, 78, 169–172.

Sandland, G.J. & Minchella, D.J. (2003). Effects of Diet and *Echinostoma revolutum* Infection on Energy Allocation Patterns in Juvenile Lymnaea elodes Snails. *Oecologia*, 134, 479–486.

Sato, T., Watanabe, K., Kanaiwa, M., Niizuma, Y., Harada, Y. & Lafferty, K.D. (2011). Nematomorph parasites drive energy flow through a riparian ecosystem. *Ecology*, 92, 201–207.

Schröder, A., van Leeuwen, A. & Cameron, T.C. (2014). When less is more: positive population-level effects of mortality. *Trends Ecol. Evol.*, 29, 614–624.

Seppälä, O., Liljeroos, K., Karvonen, A. & Jokela, J. (2008). Host condition as a constraint for parasite reproduction. *Oikos*, 117, 749–753.
Sheldon, B.C. & Verhulst, S. (1996). Ecological immunology: costly parasite defences and trade-offs in evolutionary ecology. *Trends Ecol. Evol.*, 11, 317–321.
Sokolow, S.H., Huttinger, E., Jouanard, N., Hsieh, M.H., Lafferty, K.D., Kuris, A.M. *et al.* (2015). Reduced transmission of human schistosomiasis after restoration of a native river prawn that preys on the snail intermediate host. *Proc. Natl Acad. Sci. USA*, 112, 9650–9655.
Théron, A. (1981a). Dynamics of larval populations of *Schistosoma mansoni* in *Biomphalaria glabrata* II: chronobiology of the intramolluscal larval development during the shedding period. *Ann. Trop. Med. Parasitol.*, 75, 547–554.
Théron, A. (1981b). Dynamics of larval populations of *Schistosoma mansoni* in *Biomphalaria glabrata*: I Rhythmic production of cercariae in monomiracidial infections. *Ann. Trop. Med. Parasitol.*, 75, 71–77.
Théron, A., Rognon, A., Gourbal, B. & Mitta, G. (2014). Multi-parasite host susceptibility and multi-host parasite infectivity: a new approach of the *Biomphalaria glabrata*/*Schistosoma mansoni* compatibility polymorphism. *Infect. Genet. Evol.*, 26, 80–88.
Wolfe, N.D., Dunavan, C.P. & Diamond, J. (2007). Origins of major human infectious diseases. *Nature*, 447, 279–283.
Zahoor, Z., Davies, A.J., Kirk, R.S., Rollinson, D. & Walker, A.J. (2008). Disruption of ERK signalling in *Biomphalaria glabrata* defence cells by *Schistosoma mansoni*: implications for parasite survival in the snail host. *Dev. Comp. Immunol.*, 32, 1561–1571.
Zipkin, E.F., Kraft, C.E., Cooch, E.G. & Sullivan, P.J. (2009). When can efforts to control nuisance and invasive species backfire? *Ecol. Appl.*, 19, 1585–1595.

SUPPORTING INFORMATION

Additional Supporting Information may be found online in the supporting information tab for this article.

Editor, Frida Ben-Ami
Manuscript received 29 June 2017
First decision made 4 August 2017
Second decision made 3 November 2017
Third decision made 12 February 2018
Manuscript accepted 13 February 2018